Supplementary material: Micromagnetics of magnetic chemical modulations in soft-magnetic cylindrical nanowires

L. Álvaro-Gómez,[1,2,3,4,*] S. Ruiz-Gómez,[5,6] C. Fernández-González,[3,4] M. Schöbitz,[1,2,7] N. Mille,[8] J. Hurst,[1] D. Tiwari,[1] A. De Riz,[1] I.M. Andersen,[9] J. Bachmann,[10,11] L. Cagnon,[2] M. Foerster,[5] L. Aballe,[5] R. Belkhou,[8] J.C Toussaint,[2] C. Thirion,[2] A. Masseboeuf,[1] D. Gusakova,[1] L. Pérez,[3,4,†] and O. Fruchart[1,‡]

[1] *Univ. Grenoble Alpes, CNRS, CEA, Grenoble INP, SPINTEC, 38000 Grenoble, France.*
[2] *Univ. Grenoble Alpes, CNRS, Institut Néel, 38000 Grenoble, France.*
[3] *IMDEA Nanociencia, Campus de Cantoblanco, 28049 Madrid, Spain.*
[4] *Dpto. de Física de Materiales, Universidad Complutense de Madrid, 28040 Madrid, Spain.*
[5] *Alba Synchrotron Light Facility, CELLS, 08290 Cerdanyola del Vallès, Barcelona, Spain.*
[6] *Max Planck Institute for Chemical Physics of Solids, 01187 Dresden, Germany.*
[7] *Friedrich-Alexander Univ. Erlangen-Nürnberg, Inorganic Chemistry, Erlangen, Germany.*
[8] *Synchrotron SOLEIL, l'Orme des Merisiers, Saint-Aubin, FR-91192 Gif-sur-Yvette Cedex, France.*
[9] *Centre d'Elaboration de Materiaux et d'Etudes Structurales, 31055, Toulouse, France.*
[10] *Friedrich-Alexander Univ. Erlangen-Nürnberg, Inorganic Chemistry, Erlangen, Germany*
[11] *Institute of Chemistry, Saint-Petersburg State Univ., St. Petersburg, Russia.*

(Dated: August 2, 2022)

X-ray absorption spectroscopy: correlation between experiments and theory

There is not direct correlation between the value of magnetic contrast and direction of magnetization since the absorption of x-rays follows an exponential behavior based on Beer-Lambert law:

$$I(x) = I_0 \exp\left[-\mu t(x)\right] \tag{1}$$

where $I(x)$ is the intensity of the transmitted x-rays through a material, $t(x)$ the thickness of the material and μ the absorptivity coefficient. Moreover, the experiments have a finite resolution or spot size that needs to be considered. It can be modeled by a Gaussian:

$$I_{\text{spot}}(x) = \exp\left(-x^2/2\sigma^2\right) \tag{2}$$

where σ is the standard deviation of the Gaussian, which is a measurement of the spot size. To extract quantitative information of the experimental data we have developed a post-processing code. Several approaches were followed to determine the absorptivity coefficient at the modulation $\mu_{\text{Fe}_{80}\text{Ni}_{20}}$ related to this particular experiment. The main issue to face is the fact that magnetization is not uniform across the modulation and thus the component of the magnetization along the x-ray beam ($\hat{\mathbf{k}} \cdot \mathbf{m}$) is unknown. To solve this, we decided to consider the theoretical value $\mu_{\text{th,Fe}_{80}\text{Ni}_{20}}$ and extract the background signal associated to experimental limitations. For this, we calculate the background signal, $I_{\text{b,XAS}}$, by subtracting the minimum value of the experimental profile of the transmitted intensity from the minimum calculated theoretically (black and red curve in Fig. 1a). Then we add $I_{\text{b,XAS}}$ value to the theoretical intensity (Fig. 1b). To extract the spot size, a convolution of the theoretical profile with a Gaussian of unknown width was done followed by a fit with the experimental data (Fig. 1c). In this specific case, $\sigma = 12$ nm was obtained.

The calculation of the curling angle $\theta(R)$ from the magnetic contrast of the images was done using the post processing code describe in [1] where the input parameters were the wire diameter (130 nm), μ, σ, the sample rotation ($\alpha = \beta = 10°$) and the background signal. In this case the background signal was determined by $I_{\text{b,XMCD}} = I_{\text{b,XAS}} \times I_{\text{XMCD,out}}$ where $I_{\text{XMCD,out}}$ is the XMCD intensity out of the wire. The theoretical absorptivity coefficients used were $\mu_{\text{Fe}_{65}\text{Ni}_{35}} = 0.045$ nm^{-1} and $\Delta\mu_{\text{Fe}_{65}\text{Ni}_{35}} = 0.026$ nm^{-1}. In this case, a curling angle of $\theta(R) = 32°$ for 50 mT of axial magnetic field was extracted. Furthermore, the r^2 for this fit is 0.94.

* laualv10@ucm.es
† lucas.perez@ucm.es
‡ olivier.fruchart@cea.fr

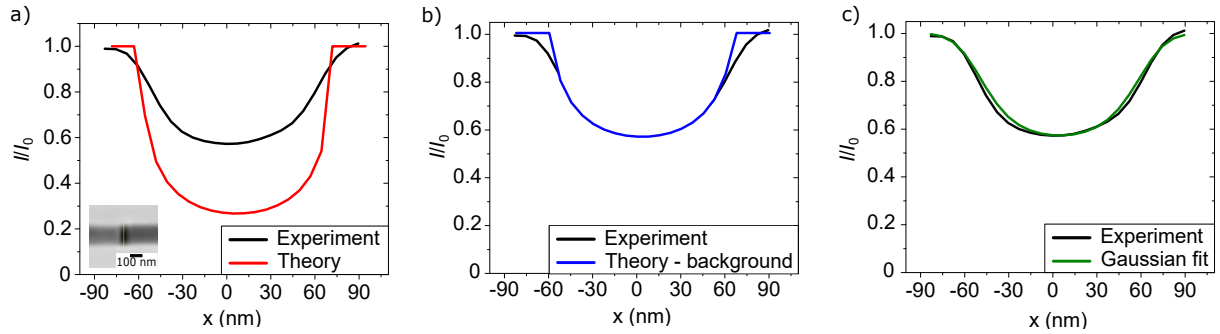

FIG. 1. Analysis of XAS and XMCD reconstructed ptychographic image to extract the spot size and curling angle. a) XAS normalized intensity profile across the cross-section of the modulation for a nanowire with $d = 130\,\text{nm}$ and $\ell = 60\,\text{nm}$ obtained experimentally (black curve). Yellow line in the inset shows the location of the line profile. The theoretical transmitted intensity is plotted by the red curve. b) Theoretical transmitted intensity after subtracting the background signal (blue) vs experimental data (black). c) Theoretical data in b) convoluted with a Gaussian whose width ($\sigma = 12$ nm) results from the fit with the experimental data.

Calculation of the current density switching threshold

A method based on the scaling of a parameter was used to determine the minimum current density to switch the circulation at the modulation from micromagnetic simulations. We have used the critical time τ_c to switch above the threshold as parameter . Before this, a criterion to define τ_c needs to be set. In Fig. 2a, the time evolution of the the maximum and minimum values of a line profile at the surface of the wire of m_z, m_ρ and m_ϕ are plotted. In this specific case, the system was a nanowire with $d = 90\,\text{nm}$ and $\ell = 60\,\text{nm}$ and $j = 3 \times 10^{12}\,\text{A/m}^2$. We decided to determine τ_c as the time when the azimuthal component changes its sign which is at $\max(m_\phi) = 0$ (orange circle in Fig. 2a). The extraction of τ_c was done by doing a linear fit between the values before and after $\max(m_\phi) = 0$ (Fig. 2b). This procedure was applied for several values of j_c to obtain several values of τ_c. The threshold current density corresponds to the j value for τ_c^{-1}=0 and can be obtained by plotting τ_c^{-1} as a function of j_c (see Fig. 2c).

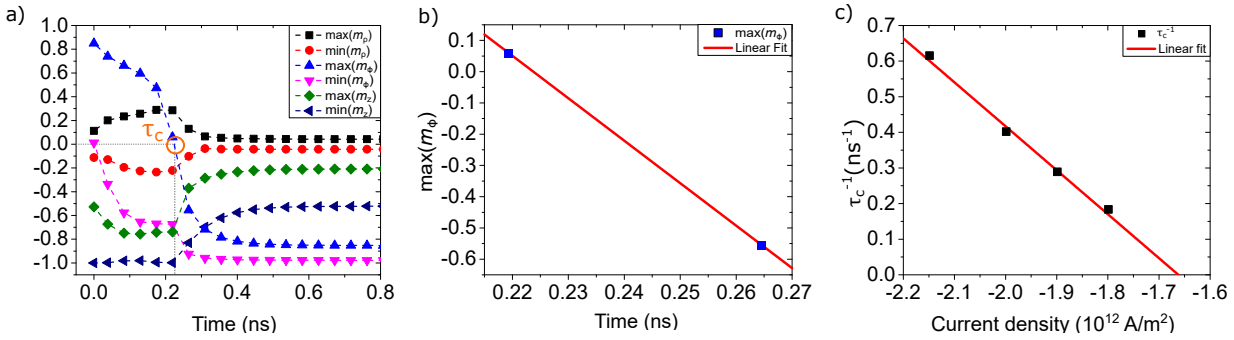

FIG. 2. Method to extract threshold current density of switching. a) Maximum and minimum value of m_z, m_ρ and m_ϕ plotted over time of a line profile at the surface of the wire before and after the switching of the circulation. The nanowire diameter is $d = 90\,\text{nm}$ and $\ell = 60\,\text{nm}$ and the current density $j = 3 \times 10^{12}\,\text{A/m}^2$. The switching time τ_c is determined by $\max(m_\phi) = 0$. b) Linear interpolation between the values before and after $\max(m_\phi) = 0$ to extract exact value of τ_c. c) Linear interpolation of the values of τ_c^{-1} as a function of j_c. Interception with the horizontal axis gives the threshold current density.

Identification of two switching regimes

The switching of circulation driven by the Œrsted field associated to a current pulse can occur at two different regimes, in the first regime the reversal is a coherent process throughout the modulation and in the second regime it is not coherent since the switching starts at the center of the modulation. The identification of the value of ℓ limiting both regimes was set by the maximum threshold current density, $j_{c,th}$, needed for reversal. This occurred at $\ell = 40\,\text{nm}$ for $d = 90\,\text{nm}$ wire and at $\ell = 30\,\text{nm}$ for $d = 130\,\text{nm}$ wire. However, since $j_{c,th}$ values for these modulation lengths

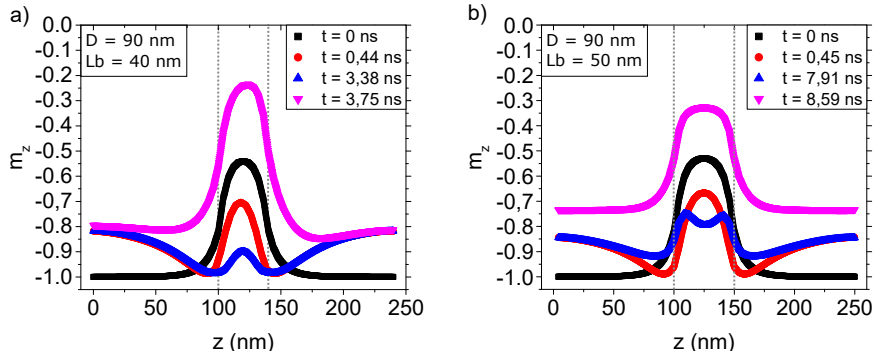

FIG. 3. Axial magnetization evolution during the switching mechanism. a) First regime: m_z vs z profiles over time at the surface of a nanowire of $d = 90\,\text{nm}$ and $\ell = 40\,\text{nm}$ under the application of a current pulse $j = -2.10 \times 10^{12}\,\text{A/m}^2$. The grey dashed lines set the location of the modulation. The profile in pink shows m_z after the reversal to a circulation parallel to the Œrsted field. b) Second regime: same as in a) for nanowire of $d = 90\,\text{nm}$ and $\ell = 50\,\text{nm}$ under the application of a current pulse $j = -1.9 \times 10^{12}\,\text{A/m}^2$.

are quite similar we decided to look in more detail the switching mechanism. For this, we analyzed over time the m_z profiles along the axial direction at the periphery of the wire. For the case of the first regime (short modulation lengths), the peak of the profile decreases homogeneously. This is shown in Fig. 3a for a nanowire of $d = 90\,\text{nm}$ and $\ell = 40\,\text{nm}$. The black curve corresponds to the m_z profile at rest, then the red and blue curve are the profiles while injecting a pulse of $j = -2.10 \times 10^{12}\,\text{A/m}^2$ and the pink curve refers to the profile under the same pulse but after the reversal of the circulation. The tilt of the Permalloy domains by the Œrsted field can be observed. Also the location of the modulation is set by the grey dashed lines. The same situation is explored in Fig. 3b for a nanowire of $d = 90\,\text{nm}$ and $\ell = 50\,\text{nm}$ under the application of a pulse of amplitude $j = -1.9 \times 10^{12}\,\text{A/m}^2$. In this case, the m_z profile before switching (blue curve) reaches its minimum at the center of the modulation. We observed this shape of the profile for $\ell \geq 50\,\text{nm}$, which sets a criteria to correlate a switching mechanism within the second regime.

Current density calculation from oscilloscope

Calculating the current density that flows trough the wire is a crucial step in the analysis of the experiments. To do so, the transmission, t, and attenuation, β, coefficients need to be calculated from the output voltage from the pulse generator V_{output}, the reflected voltage from the sample $V_{\text{reflected}}$ and the transmitted voltage trough the sample $V_{\text{transmitted}}$. The voltage, both output and reflected/transmitted, measured through 50 Ohm (either tranmission cable or end load), are directly proportional to the current. These coefficients are described as:

$$t = \frac{V_{\text{transmitted}}}{V_{\text{transmitted}} + V_{\text{reflected}}} \tag{3}$$

$$\beta = \frac{V_{\text{transmitted}} + V_{\text{reflected}}}{V_{\text{output}}} \tag{4}$$

As an example, Fig. 4 shows the voltage evolution over time for a 10 ns pulse show $V_{\text{output}} = 8.5\,\text{V}$, $V_{\text{reflected}} = 6.25\,\text{V}$ and $V_{\text{transmitted}} = 1.25\,\text{V}$, which results in $t = 0.17$ and $\beta = 0.88$. The decrease and increase over time in the transmitted and reflected signal is due to the increase of temperature due to Joule heating that changes the electrical resistance of the wire. We consider that the dynamics of our events happens within the first nanoseconds and we always consider the maximum transmitted signal accordingly. This nanowire had the following properties $d = 135\,\text{nm}$, length $= 17\,\text{um}$, resistance $R = 282\,\Omega$ and resistivity $\rho = 23\,\mu\Omega \cdot \text{cm}$. The associated current density is $j = V_{\text{transmitted}}/(\sqrt{\beta} \times A \times R_{\text{osciloscope}}) = 1.25\,\text{V}/(0.94 \times 14314\,\text{nm}^2 \times 50\,\Omega) = 1.86 \times 10^{12}\,\text{A/m}^2$. It is important to take into account that the value of β strongly depends on the setup used for each experiment ($\beta = 0.30$ for the PEEM setup used in this work) and it is crucial to consider the appropriate value for the calculation of the real current density.

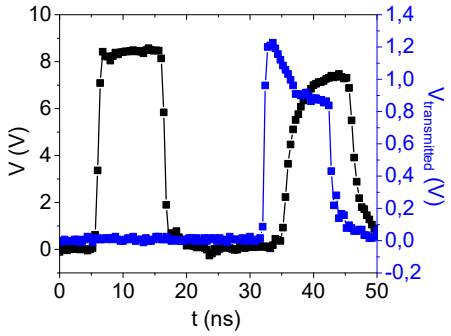

FIG. 4. Characterization of a 10 ns current pulse trough a nanowire of $d = 135\,\text{nm}$, length $= 17\,\text{um}$, resistance $R = 282\,\Omega$ and resistivity $\rho = 23\,\mu\Omega \cdot \text{cm}$. The black curve shows an output voltage of $V_{\text{output}} = 8.5\,\text{V}$ and reflected voltage $V_{\text{reflected}} = 6.25\,\text{V}$. The blue curve shows a transmitted voltage of $V_{\text{transmitted}} = 1.25\,\text{V}$.

Case of lower magnetization at the chemical modulation

In this manuscript we have not considered the case of a chemical insertion of lower magnetization since, for this situation the physics is significantly different. However, we would like to address in this section the magnetic charges distribution for the case where $M_2 < M_1$. In this situation, a nanowire with positive axial magnetization as represented by the red arrows in Fig. 5 a) have positive surface charges ($\sigma = \pm(M_2 - M_1)$) and positive volume charge distribution ($\rho = -\frac{\partial M_z(z)}{\partial z}$) at the first interface. At the second interface both magnetic charges have negative sign. The equality in sign of the magnetic charges implies that no screening mechanism can occur in this system and thus no curling magnetization driven by it. This situation resembles the one at the termination of a wire where part of the surface charges are converted in volume charges of the same sign that extend to a certain axial distance instead of just at the interface, leading to a curling state and a decrease of the dipolar energy [2].

For the case of a finite lower magnetization chemical modulation, the repulsion between magnetic charges would extend the cloud of magnetic volume charges outwards of the chemical modulation. In Fig. 5 a) the schematics of charges can be observed. In this case axial magnetization would appear at the modulation and curling magnetization next to the interfaces. Axial magnetization at the modulation is allowed due to the apperance of volume charges of opposite sign that screen the surface charges. Fig. 5 b) shows micromagnetic simulations of the micromagnetic state at rest of a 90 nm diameter $Fe_{80}Ni_{20}$ nanowire with a 100 nm long $Fe_{20}Ni_{80}$ chemical modulation. The color code represents the value of axial magnetization and the arrows the direction of magnetization. Axial magnetization at the $Fe_{20}Ni_{80}$ modulation and curling magnetization at the interfaces is confirmed.

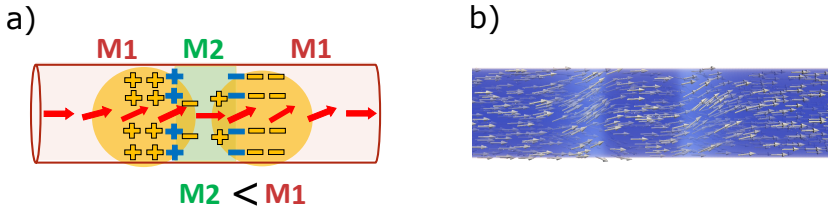

FIG. 5. a) Scheme of magnetic charges distribution for a chemical modulation of lower magnetization ($M_2 < M_1$). Surface and volume charges are represented in blue and yellow respectively. Red arrows represent magnetization direction. b) Micromagnetic simulations of a 90 nm diameter $Fe_{80}Ni_{20}$ nanowire with a 100 nm long $Fe_{20}Ni_{80}$ chemical modulation. White arrows represent magnetization direction and colorcode axial magnetization.

[1] M. Schöbitz, S. Finizio, A. D. Riz, J. Hurst, C. Thirion, D. Gusakova, J.-C. Toussaint, J. Bachmann, J. Raabe, and O. Fruchart, Time-resolved imaging of œrsted field induced magnetization dynamics in cylindrical magnetic nanowires, Appl. Phys. Lett. **118**, 172411 (2021).

[2] A. S. Arrott, B. Heinrich, T. L. Templeton, and A. Aharoni, Micromagnetics of curling configurations in magnetically soft cylinders, J. Appl. Phys. **50**, 2387 (1979).